1dflameV2: User's Guide

Raymond Speth

September 28, 2009

1 Introduction

The purpose of this document is to provide a detailed, up-to-date description of the RGD one-dimensional flame code. The code simulates an unsteady, quasi-one dimensional flame subjected to arbitrarily varying strain rate and curvature. The code is written in C++, utilizing Cantera to compute chemical properties, and the Sundials IDA solver to integrate the system of governing equations.

2 Flame Model

The elemental flame model consists of a laminar flame stabilized in a stagnation flow. The parameters of the stagnation flow may be imposed explicitly, or provided through coupling with an outer flow within which the elemental flame is embedded. The kinematics of the coupling between the elemental flame and the outer flow has been described elsewhere [2]. Here, the flame is parameterized by the strain rate and position (radius) of the stagnation point in the non-reacting flow. The stagnation flow models are described in Section 2.1.

The general 3D conservation equations for mass, momentum, energy and chemical species are reduced to one dimension by using a boundary layer approximation across the flame. The derivation of these governing equations is contained in Section 2.2.

The boundary conditions for the elemental flame model are discussed in Section 2.3.

2.1 Flame Models

2.1.1 Single Opposed-Jet Flame

The simplest configuration for the elemental flame is that of the single opposed-jet flame [2, 3]. Fluid flows from $x = \pm\infty$ toward the stagnation point at $x = 0$. The potential flow velocity field for the non-reacting flow is

$$u = a(t)z \qquad v = -a(t)x \tag{1}$$

where u and v are the velocity components in the z and x directions, respectively, and $a(t)$ is the time varying strain rate parameter. If we take the mixture coming from $x = -\infty$ to be premixed reactants and the mixture coming from $x = -\infty$ to be the reaction products, a flame will be established at some point $x < 0$ where the consumption speed balances the local fluid velocity. This configuration is shown in Figure 1. Note that a flame in this configuration can never be completely extinguished because there will always be a region of contact between reactants and products.
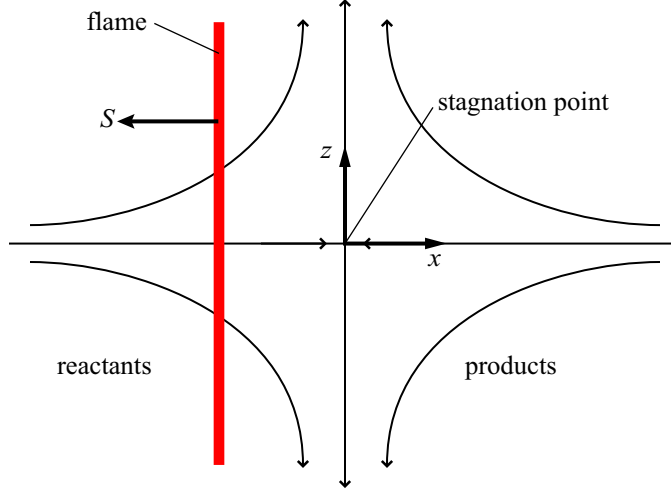
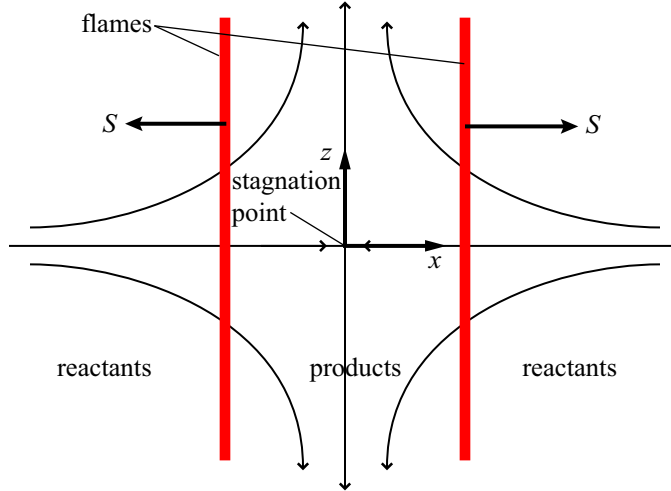Figure 1: The single opposed-jet flame configuration.

Figure 2: Twin opposed-jet flame configuration.

2.1.2   Twin Opposed-Jet Flame

The potential flow velocity field for the twin opposed-jet flame is identical to that of the single opposed jet flame, but with both inlet streams consisting of premixed reactants. As depicted in Figure 2, two flames are established, one on each side of the stagnation point, propagating away from one another. Reaction products exist in the region between the two flames. Because the composition of the products mixture is not imposed externally, this configuration allows flame extinction to occur when the flames are pushed close together. The domain is symmetric about the stagnation plane $x = 0$, allowing this configuration to be simulated numerically as a single flame with a symmetry boundary condition applied on the products side of the flame.

2.1.3   Tubular Flame at Zero Stagnation Radius

The curved flame at zero stagnation radius is quite similar to the twin opposed-jet flame. Instead of the planar stagnation flow, we have an axisymmetric stagnation flow, with reactants flowing inward
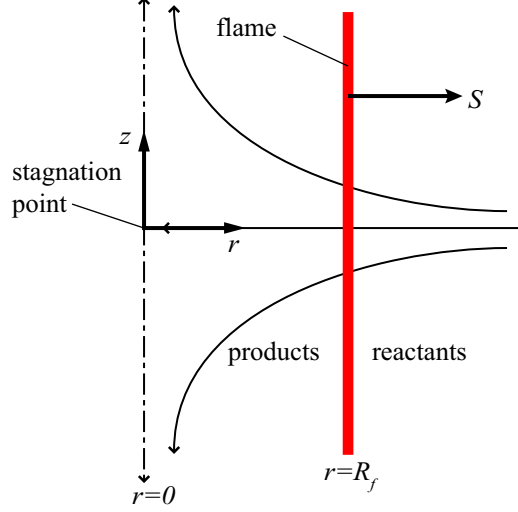
Figure 3: Tubular flame at zero stagnation radius.

from $r = \infty$ toward the stagnation point at $r = 0$, establishing a cylindrical flame propagating away from the centerline. This configuration is shown in Figure 3. The potential flow velocity field is

$$u = a(t)z \qquad v = -\frac{1}{2}a(t)r \tag{2}$$

where u and v are the velocity components in the z and r directions, respectively. As in the twin opposed jet flame, a symmetry boundary condition applies at $r = 0$, and flame extinction occurs when the flame is pushed too close to the centerline.

2.1.4 Tubular Flame at Finite Stagnation Radius

The tubular flame at zero stagnation radius can be modified by introducing a line source at $r = 0$. This produces a potential flow where the stagnation surface is a cylinder of radius R, as shown in Figure 4. Since the composition of the flow coming from $r = 0$ may be freely specified, this configuration permits both positively and negatively curved flames. The resulting potential flow velocity field is

$$u = az \qquad v = \frac{a}{2}\left(\frac{R^2 - r^2}{r}\right) \tag{3}$$

The boundary condition at $r = 0$ requires special attention in order to capture both the symmetry condition and the effect of the mass flux at the centerline. The appropriate equations for the boundary condition are derived in Section 2.3.

2.1.5 Unified Formulation

The stagnation point flow configurations discussed above can be rewritten in a unified form, permitting both planar and curved geometry through the introduction of the parameter α where $\alpha = 0$ for planar geometry and $\alpha = 1$ for curved geometry. Introducing the coordinate system (r, z) where r is the coordinate normal to the flame (regardless of whether the coordinate system is curved or planar) and the z coordinate is tangential to the flame. The potential flow velocity field
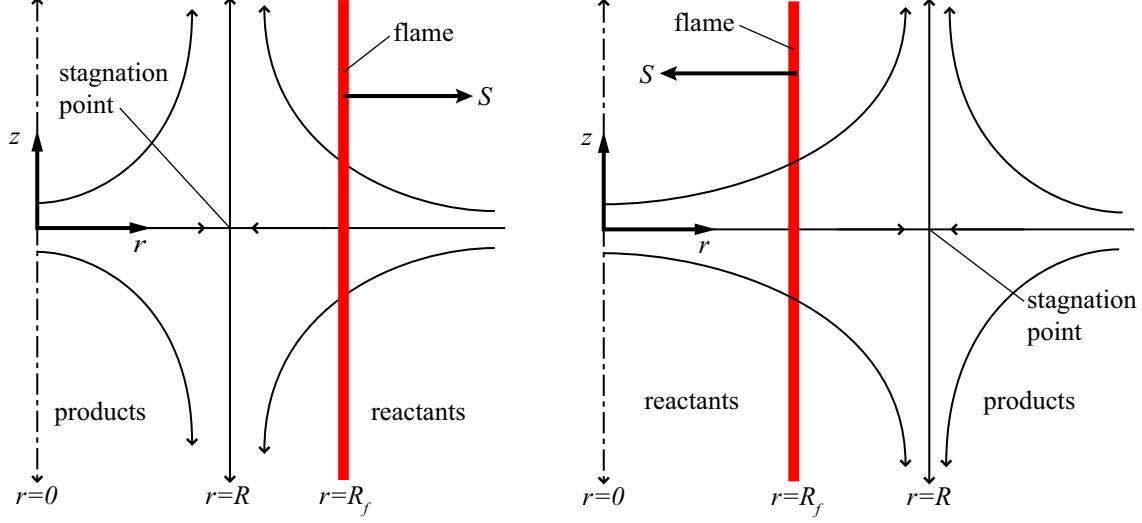
3

Figure 4: Positively (left) and negatively (right) curved tubular flames at finite stagnation radii.

is then

$$u = az \qquad v = \frac{a}{\alpha + 1}\left(\frac{|R|\,R^\alpha - r^{\alpha+1}}{r^\alpha}\right) \qquad (4)$$

This formulation permits the use of a fictitious negative stagnation point radius R, with the centerline acting as a sink rather than a source.

The stretch rate κ for a flame at radius R_f is

$$\kappa = a + \frac{\alpha}{R_f}\frac{dR_f}{dt} \qquad (5)$$

When the flame is stationary, the stretch rate reduces to $\kappa = a$ and thus curvature does not contribute to flame stretch for stationary flames in this configuration.

2.2 Governing Equations

The one-dimensional governing equations for the elemental flame are derived in this section. We begin with the general 3D governing equations for reacting flow as given by Kee [1] and reduce them to a single dimension normal to the flame using a boundary layer approximation and solving along the stagnation streamline $z = 0$. Consider the coordinate system (z, r, θ) with velocity components (u, v, w) and let $\hat{r}$ be the flame normal. We may allow this coordinate system to be either Cartesian or cylindrical through the introduction of a parameter α, where $\alpha = 1$ for the cylindrical case and $\alpha = 0$ for the Cartesian case. In making the boundary layer approximation, the tangential variations of all quantities except the pressure p and tangential velocity u are neglected. The velocity and all variations in the θ direction are zero. For an arbitrary scalar F, the gradient and substantial derivative are defined as

$$\nabla F \equiv \hat{z}\frac{\partial F}{\partial z} + \hat{r}\frac{\partial F}{\partial r} \qquad (6)$$

$$\frac{DF}{Dt} = \frac{\partial F}{\partial t} + \mathbf{v}\cdot\nabla F = \frac{\partial F}{\partial t} + u\frac{\partial F}{\partial z} + v\frac{\partial F}{\partial r} \qquad (7)$$

4

The divergence of a vector $\mathbf{F}$ is defined as

$$\nabla \cdot \mathbf{F} \equiv \frac{\partial F_z}{\partial z} + \frac{1}{r^\alpha} \frac{\partial}{\partial r} (r^\alpha F_r) \tag{8}$$

where F_z and F_r are respectively the z and r components of $\mathbf{F}$.

2.2.1 Momentum Equation

First, we will focus on the momentum equation. In general three-dimensional form, it is

$$\rho \frac{D\mathbf{v}}{Dt} = \mathbf{f} + \nabla \cdot \mathsf{T} \tag{9}$$

where T is the stress tensor,

$$\mathsf{T} = \begin{pmatrix} -p + 2\mu \frac{\partial u}{\partial z} + \kappa \nabla \cdot \mathbf{v} & \mu \left(\frac{\partial u}{\partial r} + \frac{\partial v}{\partial z} \right) & \mu \left(\frac{1}{r^\alpha} \frac{\partial u}{\partial \theta} + \frac{\partial w}{\partial z} \right) \\ \mu \left(\frac{\partial u}{\partial r} + \frac{\partial v}{\partial z} \right) & -p + 2\mu \frac{\partial v}{\partial r} + \kappa \nabla \cdot \mathbf{v} & \mu \left(\frac{\partial w}{\partial r} - \alpha \frac{w}{r} + \frac{1}{r^\alpha} \frac{\partial v}{\partial \theta} \right) \\ \mu \left(\frac{1}{r^\alpha} \frac{\partial u}{\partial \theta} + \frac{\partial w}{\partial z} \right) & \mu \left(\frac{\partial w}{\partial r} - \alpha \frac{w}{r} + \frac{1}{r^\alpha} \frac{\partial v}{\partial \theta} \right) & -p + 2\mu \left(\frac{1}{r^\alpha} \frac{\partial w}{\partial \theta} + \alpha \frac{v}{r} \right) + \kappa \nabla \cdot \mathbf{v} \end{pmatrix} \tag{10}$$

and the body force $\mathbf{f} = \mathbf{0}$. Here, p is the pressure and μ is the dynamic viscosity of the mixture. Setting velocities and derivatives in the θ direction to zero, the z-momentum equation is

$$\rho \frac{\partial u}{\partial t} + \rho u \frac{\partial u}{\partial z} + \rho v \frac{\partial u}{\partial r} = \frac{\partial}{\partial z} \left[-p + 2\mu \frac{\partial u}{\partial z} + \kappa \nabla \cdot \mathbf{v} \right] + \frac{1}{r^\alpha} \frac{\partial}{\partial r} \left[r^\alpha \mu \left(\frac{\partial u}{\partial r} + \frac{\partial v}{\partial z} \right) \right] \tag{11}$$

The term containing the second coefficient of viscosity, $\kappa \nabla \cdot \mathbf{v}$, is taken to be zero. Additionally, $\partial v / \partial z$ and $\partial^2 u / \partial z^2$ are neglected by the boundary layer approximation, giving the simplified z-momentum equation

$$\rho \frac{\partial u}{\partial t} + \rho u \frac{\partial u}{\partial z} + \rho v \frac{\partial u}{\partial r} = -\frac{\partial p}{\partial z} + \frac{1}{r^\alpha} \frac{\partial}{\partial r} \left[r^\alpha \mu \frac{\partial u}{\partial r} \right] \tag{12}$$

The pressure gradient outside the boundary layer may be obtained by substituting the potential flow solution for u and v into the momentum equation.

$$\rho_\infty z \frac{da}{dt} + \rho_\infty a^2 z = -\frac{\partial p}{\partial z} \tag{13}$$

where ρ_∞ is the density of the reactants mixture. By the boundary layer approximation, this must be the pressure gradient inside the boundary layer as well.

The z dependence of u may be found similarly.

$$\rho \frac{\partial u}{\partial t} + \rho u \frac{\partial u}{\partial z} + \rho v \frac{\partial u}{\partial r} = \rho_\infty z \frac{da}{dt} + \rho_\infty a^2 z + \frac{1}{r^\alpha} \frac{\partial}{\partial r} \left[r^\alpha \mu \frac{\partial u}{\partial r} \right] \tag{14}$$

Now, introduce the notation $U \equiv ua/u_\infty$. Using equation 4, we can then write

$$u = \frac{U u_\infty}{a} = \frac{U a z}{a} = U z \tag{15}$$

Substituting this into the momentum equation gives

$$\rho z \frac{\partial U}{\partial t} + \rho U z \left(z \frac{\partial U}{\partial z} + U \right) + \rho v z \frac{\partial U}{\partial r} = \rho_\infty z \frac{da}{dt} + \rho_\infty a^2 z + \frac{z}{r^\alpha} \frac{\partial}{\partial r} \left[r^\alpha \mu \frac{\partial U}{\partial r} \right] \tag{16}$$

Dividing by az, and solving along the stagnation streamline $z = 0$, the momentum equation simplifies to

$$\rho \frac{\partial U}{\partial t} + \rho U^2 + \rho v \frac{\partial U}{\partial r} = \rho_\infty \frac{da}{dt} + \rho_\infty a^2 + \frac{1}{r^\alpha} \frac{\partial}{\partial r} \left[r^\alpha \mu \frac{\partial U}{\partial r} \right] \tag{17}$$

5

2.2.2 Continuity Equation

Now consider the mass conservation equation

$$\frac{\partial \rho}{\partial t} + \nabla \cdot (\rho \mathbf{v}) = 0 \tag{18}$$

Expanding the divergence using Equation 8 gives

$$\frac{\partial \rho}{\partial t} + \frac{1}{r^\alpha}\frac{\partial}{\partial r}\left(r^\alpha \rho v\right) + \rho\frac{\partial u}{\partial z} = 0 \tag{19}$$

Making the substitution for the similarity variable U, the mass conservation equation becomes

$$\frac{\partial \rho}{\partial t} + + \frac{1}{r^\alpha}\frac{\partial}{\partial r}\left(r^\alpha \rho v\right) + \rho U = 0 \tag{20}$$

2.2.3 Species Equation

The general form of the species continuity equation is

$$\rho\frac{DY_k}{Dt} = -\nabla \cdot \mathbf{j}_k + \dot{\omega}_k W_k \tag{21}$$

where Y_k is the mass fraction of species k, $\dot{\omega}_k$ is the molar production rate of species k, W_k is the molecular weight of species k, and the diffusion mass flux $\mathbf{j}_k$ is defined as

$$\mathbf{j}_k = -\frac{\rho W_k}{\bar{W}}D_{km}\nabla X_k - \frac{D_k^T}{T}\nabla T + Y_k\mathbf{j}' \tag{22}$$

$$-\rho D_{km}\left(\nabla Y_k + \frac{Y_k}{\bar{W}}\nabla\bar{W}\right) - \frac{D_k^T}{T}\nabla T + Y_k\mathbf{j}' \tag{23}$$

Here, T is the temperature, X_k are the species mole fractions, and D_{km} and D_k^T are respectively the mixture-averaged diffusion coefficient and the thermal diffusion coefficient of species k. Note that this definition of the diffusion mass flux includes the thermal diffusion (Soret) effect. The final term introduces a correction, $\mathbf{j}'$, which corrects for the inaccuracy of mixture-averaged model so that the requirement $\sum \mathbf{j}_k = 0$ is satisfied. In order to calculate $\mathbf{j}'$, we first calculate the diffusion mass fluxes ignoring its contribution

$$\mathbf{j}_k^* = -\rho D_{km}\left(\nabla Y_k + \frac{Y_k}{\bar{W}}\nabla\bar{W}\right) - \frac{D_k^T}{T}\nabla T \tag{24}$$

Then, $\mathbf{j}'$ is calculated as

$$\mathbf{j}' = -\sum_k \mathbf{j}_k^* \tag{25}$$

Substituting the gradient, substantial derivative and divergence as defined in equations 6, 7 and 8, respectively, and setting the z-derivatives to zero, the species equation becomes

$$\rho\frac{\partial Y_k}{\partial t} + V\frac{\partial Y_k}{\partial r} = -\frac{1}{r^\alpha}\frac{\partial}{\partial r}\left[r^\alpha j_k\right] + \dot{\omega}_k W_k \tag{26}$$

and the diffusion mass flux is

$$j_k = -\rho D_{km}\left(\frac{\partial Y_k}{\partial r} + \frac{Y_k}{\bar{W}}\frac{\partial\bar{W}}{\partial r}\right) - \frac{D_k^T}{T}\frac{\partial T}{\partial r} + Y_k j' \tag{27}$$

6

2.2.4 Energy Equation

Finally we turn our attention to the energy conservation equation. The general form of the energy equation, expressed in terms of the enthalpy, is

$$\rho \frac{Dh}{Dt} = \frac{Dp}{Dt} - \nabla \cdot \mathbf{q} + \Phi \tag{28}$$

where h is the enthalpy, q is the heat flux and Φ is the viscous work. By the zero-Mach-number assumption, we neglect the effect of pressure variations, so $Dp/Dt = 0$. The viscous work term is also assumed to be much smaller than the energy released by chemical reactions and is therefore neglected. Expanding the substantial derivative of the enthalpy in terms of T, Y_k and specific heat capacity c_p gives

$$\frac{Dh}{Dt} = \sum_{k=1}^{K} \left(Y_k \frac{Dh_k}{Dt} + h_k \frac{DY_k}{Dt} \right) = c_p \frac{DT}{Dt} + \sum_{k=1}^{K} h_k \frac{DY_k}{Dt} \tag{29}$$

The total number of species is K. The substantial derivative of Y_k is replaced using the species equation 21. With these substitutions, the energy equation then becomes

$$\rho c_p \frac{DT}{Dt} + \sum_{k=1}^{K} h_k \left(-\nabla \cdot \mathbf{j}_k + \dot{\omega}_k W_k \right) = -\nabla \cdot \mathbf{q} \tag{30}$$

The heat flux vector $\mathbf{q}$ is

$$\mathbf{q} = -\lambda \nabla T + \sum_{k=1}^{K} h_k j_k + \mathbf{q}_r \tag{31}$$

where λ is the thermal conductivity of the mixture and the radiation heat flux $\mathbf{q}_r$ is neglected in the present model. Also neglected is the Dufour heat flux, proportional to the gradients in species concentrations, which is typically three orders of magnitude smaller than the Fourier heat flux, $\lambda \nabla T$. Substituting the heat flux vector into the energy equation, and noting that $\hat{h}_k = h_k W_k$ where $\hat{h}_k$ is the molar enthalpy, we obtain

$$\rho c_p \frac{DT}{Dt} + \sum_{k=1}^{K} \hat{h}_k \dot{\omega}_k - \sum_{k=1}^{K} h_k \nabla \cdot \mathbf{j}_k = -\nabla \cdot \left(-\lambda \nabla T + \sum_{k=1}^{K} h_k \mathbf{j}_k \right) \tag{32}$$

By expanding the term $\nabla \cdot \left(\sum_{k=1}^{K} h_k j_k \right)$ and performing appropriate cancellations, the energy equation simplifies slightly to

$$\rho c_p \frac{DT}{Dt} + \sum_{k=1}^{K} \hat{h}_k \dot{\omega}_k + \sum_{k=1}^{K} \mathbf{j}_k \nabla \cdot h_k = \nabla \cdot (\lambda \nabla T) \tag{33}$$

Making the substitutions for the gradient, substantial derivative and divergence, and setting the z-derivatives to zero, the one-dimensional form of the energy equation is

$$\rho \frac{\partial T}{\partial t} + \rho v \frac{\partial T}{\partial r} + \frac{1}{c_p} \left(\sum_{k=1}^{K} \hat{h}_k \dot{\omega}_k + \sum_{k=1}^{K} j_k c_{p,k} \frac{\partial T}{\partial r} \right) = \frac{1}{c_p} \frac{1}{r^\alpha} \frac{\partial}{\partial r} \left[r^\alpha \lambda \frac{\partial T}{\partial r} \right] \tag{34}$$

2.2.5 Summary

Introducing the notation $V \equiv \rho v$ for the mass flux and recasting the governing equations in residual form, the final mass, momentum, species, and energy conservation equations are:

$$\frac{\partial \rho}{\partial t} + + \frac{1}{r^\alpha}\frac{\partial}{\partial r}\left(r^\alpha V\right) + \rho U = 0 \tag{35}$$

$$\rho\frac{\partial U}{\partial t} + V\frac{\partial U}{\partial r} + \rho U^2 - \rho_\infty \left(\frac{da}{dt} + a^2\right) - \frac{1}{r^\alpha}\frac{\partial}{\partial r}\left[r^\alpha \mu \frac{\partial U}{\partial r}\right] = 0 \tag{36}$$

$$\rho\frac{\partial Y_k}{\partial t} + V\frac{\partial Y_k}{\partial r} + \frac{1}{r^\alpha}\frac{\partial}{\partial r}\left[r^\alpha j_k\right] - \dot{\omega}_k W_k = 0 \tag{37}$$

$$\rho\frac{\partial T}{\partial t} + V\frac{\partial T}{\partial r} + \frac{1}{c_p}\left(\sum_{k=1}^{K}\hat{h}_k\dot{\omega}_k + \sum_{k=1}^{K}j_k c_{p,k}\frac{\partial T}{\partial r} - \frac{1}{r^\alpha}\frac{\partial}{\partial r}\left[r^\alpha \lambda \frac{\partial T}{\partial r}\right]\right) = 0 \tag{38}$$

where the diffusion mass flux appearing in the species and energy equations is defined as

$$j_k = -\rho D_{km}\frac{\partial Y_k}{\partial r} - \frac{D_k^T}{T}\frac{\partial T}{\partial r} + Y_k j' \tag{39}$$

2.3 Boundary Conditions

Establishing the boundary conditions for the elemental flame requires separate consideration of each of the flame configurations described in Section 2.1.

2.3.1 Single Opposed Jet

For the single opposed jet flame, defined in Section 2.1.1, the boundary conditions for the species and energy equations consist of defining the temperature and mass fraction of the two incoming streams. For the momentum equation, spatial gradients in U must vanish on both sides of the flame, and we solve the simplified form of the momentum equation,

$$\rho\frac{\partial U}{\partial t} + \rho U^2 - \rho_\infty \left(\frac{da}{dt} + a^2\right) = 0 \tag{40}$$

for each boundary point. For steady strain rates, this equation requires that $U = a$ on the reactants side and $U = a\sqrt{\rho_u/\rho_b}$ on the products side.

For a premixed flame with reactants supplied from $-\infty$, the boundary conditions for the species and energy equations are:

$$\begin{array}{llll} r = -\infty: & Y_k = Y_{k,u} & T = T_u \\ r = +\infty: & Y_k = Y_{k,b} & T = T_b \end{array} \tag{41}$$

The burned gas temperature and composition correspond to the unburned mixture brought to equilibrum at constant enthalpy and pressure. The boundary condition for the continuity equationis taken at the left side of the computational domain, where V is held fixed.

2.3.2 Central Control Volume

For curved flames at finite stagnation radius, or flames specified in terms of the unified formulation given in Section 2.1.5, the $r = \infty$ boundary condition is the same as for the curved flame at zero stagnation radius. The boundary conditions at $r = 0$, however, require special attention. First, the mass flux at the center must be expressed in terms of rV because $V \to \infty$ as $r \to 0$ in the potential flow solution of Equation 3. If we specify the non-reacting stagnation point radius R, then the boundary condition for the continuity equation is

$$r = 0: \quad rV = \frac{1}{\alpha + 1} \rho a \left| R \right| R \tag{42}$$

If the boundary mass flux $(rV)_0$ is positive, indicating the presence of source at the boundary, special care must be taken in specifying the boundary conditions for the energy, species and momentum equations. While the zero-gradient condition must still hold because of the symmetry at that boundary, it is important to retain the effect of the mixture being introduced, which may not be at the same state as the mixture in the vicinity of $r = 0$. To this end, we consider an integral, control volume approach to the $r = 0$ boundary condition. Beginning with the species conservation equation 37, we multiply through by r^α and integrate from 0 to some small radius R_i.

$$\int_0^{R_i} r^\alpha \rho \frac{\partial Y_k}{\partial t} + r^\alpha V \frac{\partial Y_k}{\partial r} + \frac{\partial}{\partial r} \left[r^\alpha j_k \right] - r^\alpha \dot{\omega}_k W_k \, dr = 0 \tag{43}$$

Because this volume is small, we assume that variations of Y_k, ρ and $\dot{\omega}_k$ are negligible, so the unsteady term and the production term may be taken out of the integral.

$$\frac{r^{\alpha+1}}{\alpha + 1} \left(\rho \frac{\partial Y_k}{\partial t} - \dot{\omega}_k W_k \right) + \int_0^{R_i} r^\alpha V \frac{\partial Y_k}{\partial r} + \frac{\partial}{\partial r} \left[r^\alpha j_k \right] \, dr = 0 \tag{44}$$

The convection term may be integrated by noting that variations in $r^\alpha V$ are negligible across this small distance. Furthermore, we recognize that $Y_k|_{r=0} = Y_{k,left}$ is the mass fraction corresponding to the inlet mixture (either reactants or products). The diffusion term may also be integrated, noting that $j_k|_{r=0} = 0$ by the symmetry condition. We now have an ODE for the mass fraction of species k in the vicinity of the symmetry boundary,

$$\frac{R_i^{\alpha+1}}{\alpha + 1} \left(\rho \frac{\partial Y_k}{\partial t} - \dot{\omega}_k W_k \right) + (r^\alpha V)_0 \left(Y_{k,left} - Y_k \right) + R_i^\alpha j_k = 0 \tag{45}$$

Finally, we divide by the leading coefficient so that this equation scales similarly to the species equation in the rest of the domain:

$$\rho \frac{\partial Y_k}{\partial t} - \dot{\omega}_k W_k + \frac{\alpha + 1}{R_i^{\alpha+1}} (r^\alpha V)_0 \left(Y_{k,left} - Y_k \right) + \frac{\alpha + 1}{R_i} j_k = 0 \tag{46}$$

A similar analysis for the energy equation yields

$$\rho \frac{\partial T}{\partial t} + \frac{1}{c_p} \sum_{k=1}^K \hat{h}_k \dot{\omega}_k + \frac{\alpha + 1}{R_i^{\alpha+1}} (r^\alpha V)_0 \left(T_{left} - T \right) - \frac{\alpha + 1}{R_i} R_i^\alpha \left(\lambda \frac{\partial T}{\partial r} \right) = 0 \tag{47}$$

In the case of the momentum equation, we neglect the term associated with the boundary mass flux, and obtain

$$\rho \frac{\partial U}{\partial t} + \rho U^2 - \rho_\infty \left(\frac{\partial a}{\partial t} + a^2 \right) - \frac{\alpha + 1}{R_i} \mu \frac{\partial U}{\partial r} = 0 \tag{48}$$

9

If the boundary mass flux $(rV)_0$ is negative, the term including it in each of these boundary conditions is eliminated.

2.4 Multicomponent Fuel Mixtures

In this section, the formula for the composition of the reactants mixture is derived, assuming an arbitrary fuel and oxidizer mixture and a specified equivalence ratio. It is assumed that only H, C and O are the only reacting elements present. Other elements may be present, but are assumed to be inert. Given the mole fractions of the fuel components, $X_{k,f}$, and the mole fractions of the oxidizer components, $X_{k,o}$, and the chemical formulas for each species, $C_{n_k}H_{m_k}O_{p_k}$ the number of moles of each element per mole of fuel are defined as

$$C_f = \sum_k X_{k,f} n_k \tag{49}$$

$$H_f = \sum_k X_{k,f} m_k \tag{50}$$

$$O_f = \sum_k X_{k,f} p_{k,f} \tag{51}$$

and the number of moles of each element per mole of oxidizer are C_o, H_o, and O_o, calculated similarly.

For a stoichiometric fuel/oxidizer mixture, all hydrocarbons are converted to CO_2 and H_2O. Defining F as the stoichiometric fuel/oxidizer ratio, the reaction may be written as

$$F \left(\sum_k X_{k,f} C_{n_k} H_{m_k} O_{p_k} \right) + \sum_k X_{k,o} C_{n_k} H_{m_k} O_{p_k} \rightarrow$$

$$(FC_f + C_o) CO_2 + \frac{1}{2} (FH_f + H_o) H_2O + \frac{1}{2} \left(FO_f + O_o - 2FC_f - 2C_o - \frac{1}{2} FH_f - \frac{1}{2} H_o \right) O_2 \tag{52}$$

If all the oxygen is consumed, then we can solve for F:

$$FO_f + O_o - 2FC_f - 2C_o - \frac{1}{2} FH_f - \frac{1}{2} H_o = 0 \tag{53}$$

$$F = -\frac{O_o - 2C_o - H_o/2}{O_f - 2C_f - H_f/2} \tag{54}$$

The final reactant mixture composition can be calculated using the given equivalence ratio

$$X_k = \frac{F\phi}{1 + F\phi} X_{k,f} + \frac{1}{1 + F\phi} X_{k,o} \tag{55}$$

3 Numerical Simulation

The governing equations developed in the previous section are solved numerically using an implicit finite difference method. The equations are discretized spatially on an adaptive non-uniform grid, producing a system of differential algebraic equations. The discretized equations are integrated using the Sundials IDA solver [REF]. The IDA solver integrates the equations using the variable-order

(from 1 to 5) backward differentiation formula (BDF). At each timestep, this produces a system of nonlinear algebraic equations, which are solved using a preconditioned Newton-Krylov method. Thermodynamic properties, transport coefficients, and chemical kinetic rates are calculated using the Cantera [REF] library.

3.1 Finite Difference Discretization

3.1.1 Derived Grid Parameters

It is helpful to first define a number of derived grid parameters which occur repeatedly in the discretized governing equations. Let r_j be the spatial location of each grid point. The mesh spacing h_j is then defined as

$$h_j = r_{j+1} - r_j \tag{56}$$

The coefficients $\mathbb{C}_j^-$, $\mathbb{C}_j$, and $\mathbb{C}_j^+$ are the coefficients of neighboring points in the second-order centered difference approximation to the first derivative, and are calculated as

$$\mathbb{C}_j^- = \frac{-h_j}{h_{j-1}(h_j + h_{j-1})} \tag{57}$$

$$\mathbb{C}_j = \frac{h_j - h_{j-1}}{h_j h_{j-1}} \tag{58}$$

$$\mathbb{C}_j^+ = \frac{h_{j-1}}{h_j(h_j + h_{j-1})} \tag{59}$$

A few other quantities which will are:

$$\mathbb{D}_j = \frac{1}{2}(r_{j+1} - r_{j-1}) \tag{60}$$

$$r_{j+1/2} = \frac{1}{2}(r_{j+1} + r_j) \tag{61}$$

3.1.2 Governing Equations

In this section, we will give the finite difference discretizations of the governing equations. We start with the discretizations of a number of derived quantities which are used in the formulation of the governing equations. The heat flux q is calculated between grid points as

$$q_{j+1/2} \approx -\frac{\lambda_j + \lambda_{j+1}}{2} \frac{T_{j+1} - T_j}{h_j} \tag{62}$$

Similarly, the diffusion mass fluxes are calculated as

$$j_{k,j+1/2} = -\frac{1}{2}\left(\rho_j D_{km,j} + \rho_{j+1} D_{km,j+1}\right)\frac{Y_{k,j+1} - Y_{k,j}}{h_j} - \frac{1}{2}\left(\frac{\rho_j D_{km,j} Y_{k,j}}{\bar{W}_j} + \frac{\rho_{j+1} D_{km,j+1} Y_{k,j+1}}{\bar{W}_{j+1}}\right)\frac{\bar{W}_{j+1} - \bar{W}_j}{h_j}$$

$$- \frac{1}{2}\left(\frac{D_{k,j+1}^T}{T_{j+1}} + \frac{D_{k,j}^T}{T_j}\right)\frac{T_{j+1} - T_j}{h_j} + \frac{1}{2}(Y_{k,j+1} + Y_{k,j})j'_{j+1/2} \tag{63}$$

The sum appearing in the enthalpy flux term of the energy equation is calculated as

$$S_{j+1/2} = \left(\sum_k j_k c_{p,k}\right)_{j+1/2} = \sum_k \frac{c_{p,k,j+1} + c_{p,k,j}}{2} j_{k,j+1/2} \tag{64}$$

11

Now, we will give the discretizations of each term in the energy equation; the species and momentum equations are discretized in essentially the same manner.

The unsteady term is simply

$$\left(\rho\frac{\partial T}{\partial t}\right)_j \approx \rho_j\frac{dT_j}{dt} \tag{65}$$

The convective term is discretized using a second-order centered difference approximation:

$$\left(V\frac{\partial T}{\partial r}\right)_j \approx V_j\left(\mathbb{C}_j^- T_{j-1} + \mathbb{C}_j T_j + \mathbb{C}_j^+ T_{j+1}\right) \tag{66}$$

We discretize the diffusive (conduction) term as

$$\left(\frac{1}{r^\alpha c_p}\frac{\partial}{\partial r}\left[r^\alpha q\right]\right)_j \approx \frac{1}{r_j c_{p,j}}\frac{r_{j+1/2}q_{j+1/2} - r_{j-1/2}q_{j-1/2}}{\mathbb{D}_j} \tag{67}$$

The enthalpy flux term is discretized as

$$\left(\frac{S}{c_p}\frac{\partial T}{\partial r}\right)_j \approx \frac{1}{c_{p,j}}\frac{\left(S_{j+1/2} + S_{j-1/2}\right)}{2}\left(\mathbb{C}_j^- T_{j-1} + \mathbb{C}_j T_j + \mathbb{C}_j^+ T_{j+1}\right) \tag{68}$$

The production term is simply

$$\left(\sum h_k\dot{\omega}_k\right)_j \approx \sum h_{k,j}\dot{\omega}_{k,j} \tag{69}$$

The continuity equation 35 is discretized using a first order fully implicit finite difference method. The boundary condition for the mass flux is taken at $j = 0$. The discretized form of the continuity equation is

$$\frac{d\rho_j}{dt} + \frac{r_j^\alpha V_j - r_{j-1}^\alpha V_{j-1}}{r_{j+1/2}^\alpha h_{j-1}} + \rho_j U_j = 0 \tag{70}$$

Since ρ is not one of the solution variables, we must calculate $\partial\rho/\partial t$ from the state variables T and Y_k,

$$\frac{\partial\rho}{\partial t} = \frac{\partial\rho}{\partial T}\frac{\partial T}{\partial t} + \sum_k\frac{\partial\rho}{\partial Y_k}\frac{\partial Y_k}{\partial t} \tag{71}$$

The first term can be found from the ideal gas law,

$$P = \rho\frac{\bar{R}}{\bar{W}}T \tag{72}$$

which can be rewritten as

$$\rho = \frac{P\bar{W}}{\bar{R}T} \tag{73}$$

$$\frac{\partial\rho}{\partial T} = -\frac{P\bar{W}}{RT^2} = -\frac{\rho}{T} \tag{74}$$

The derivatives of the second term are calculated similarly, based on the formula for the mixture molecular weight $\bar{W}$:

$$\bar{W} = \left[\sum_i Y_i/W_i\right]^{-1} \tag{75}$$

12

$$\frac{\partial \bar{W}}{\partial Y_k} = -\left[\sum_i Y_i/W_i\right]^{-2} \frac{1}{W_k} = -\frac{\bar{W}^2}{W_k} \tag{76}$$

$$\frac{\partial \rho}{\partial Y_k} = \frac{P}{RT} \frac{\partial \bar{W}}{\partial Y_k} = -\frac{\rho \bar{W}}{W_k} \tag{77}$$

Finally, we have

$$\frac{\partial \rho}{\partial t} = -\frac{\rho}{T} \frac{\partial T}{\partial t} - \sum \frac{\rho \bar{W}}{W_k} \frac{\partial Y_k}{\partial t} \tag{78}$$

3.1.3   Boundary Conditions

The boundary conditions must also be written as ODEs or algebraic equations. There are several different cases to consider, depending on the boundary configuration.

For boundaries where the composition and temperature are fixed, e.g. both boundaries of the free flame, or at the $r = \infty$ boundary in the twin and curved flame configurations, we have

$$\frac{dT_j}{dt} = 0 \tag{79}$$

$$\frac{dY_k}{dt} = 0 \tag{80}$$

For the momentum equation, we discretize equation 40 as

$$\rho_j \frac{dU_j}{dt} + \rho_j U_j^2 - \rho_\infty \left(\frac{da}{dt} + a^2\right) = 0 \tag{81}$$

In a few cases, a simple zero-gradient condition for T and Y_k is applied. This boundary condition is not usually consistent with the direction of the convective velocity V at the boundary, except in the special case of the unstrained flame. In these cases, the zero gradient condition (on the right-hand side of the domain) requires

$$\frac{T_J - T_{J-1}}{h_{J-1}} = 0 \tag{82}$$

$$\frac{Y_{k,J} - Y_{k,J-1}}{h_{J-1}} = 0 \tag{83}$$

where J is the index of the last grid point.

For boundary conditions at $r = 0$, discretized forms of equations 46, 47 and 48 are used. Most of the terms in these equations use the same discretization as terms elsewhere in the domain, with the exception of the diffusive term. Since we know that $\partial T/\partial r = 0$ at $r = 0$,

$$q_{j+1/2} \approx -(\lambda_j + \lambda_{j+1}) \frac{T_{j+1} - T_j}{h_j} \tag{84}$$

which is twice the value obtained normally. The same applies for the diffusive mass and momentum fluxes.

3.2 Solution of the Discretized Problem

In the previous section, we established a system of ordinary differential and algebraic equations modeling the elemental flame. We may write this system of equations generically as

$$\mathbf{f}\left(t, \mathbf{y}, \mathbf{y}'\right) = \mathbf{0} \tag{85}$$

where $\mathbf{f}$ is the system of equations, $\mathbf{y}$ is the solution vector, $\mathbf{y}' = d\mathbf{y}/dt$ and t is time. Given an initial condition, t_0, $\mathbf{y}_0$, $\mathbf{y}_0'$, the system can be integrated to find $\mathbf{y}(t_n)$ where t_n is some future time. The structure of the solution vector is

$$\mathbf{y} = [V_0, U_0, T_0, Y_{0,0}, \ldots, Y_{K,0}, \ldots \ldots, V_J, U_J, T_J, Y_{0,J}, \ldots, Y_{K,J}]^T \tag{86}$$

and the structure of the function $\mathbf{f}$ is

$$\mathbf{f} = [C_0, M_0, E_0, S_{0,0}, \ldots, S_{K,0}, \ldots \ldots, C_J, M_J, E_J, S_{0,J}, \ldots, S_{K,J}]^T \tag{87}$$

where $S_{k,j}$, E_j, M_j and C_j are the respective species, energy, momentum and continuity equations at point j. The total number of grid points is $J + 1$, and the total number of species is $K + 1$. For the boundary conditions at $j = 0$ and $j = J$, the corresponding boundary equations discussed in section 3.1.3 are used.

The nonlinear system of governing equations are solved using an inexact Newton's method coupled with an iterative sparse linear solver (Usually BiCGStab), as implemented by the Sundials IDA solver. A detailed description of the solution method is contained in the IDA User's Guide [REF]. Using the Sundials solver requires us to provide the following:

- A function to evaluate the residual function $\mathbf{f}$ given t and (estimates for) $\mathbf{y}$ and $\mathbf{y}'$.

- A preconditioner, approximating the inverse of the Jacobian $\partial \mathbf{f}/\partial \mathbf{y}$

- A consistent initial condition t_0, $\mathbf{y}_0$, $\mathbf{y}_0'$, such that $\mathbf{f}\left(t_0, \mathbf{y}_0, \mathbf{y}_0'\right) = \mathbf{0}$.

The residual function is computed using the finite difference equations derived in section 3.1. In the next two sections, we will give methods for obtaining the Jacobian components and computing a consistent initial condition.

3.3 Jacobian Components

To accelerate the convergence rate of the iterative solver, a preconditioner which approximates the inverse of the Jacobian must be supplied. Based on the construction of our finite difference stencil and the arrangement of the solution vector $\mathbf{y}$, the Jacobian has a block tridiagonal structure, e.g.

$$J = \begin{bmatrix} B_0 & C_0 & & & & & \\ A_1 & B_1 & C_1 & & & & \\ & \ddots & \ddots & \ddots & & & \\ & & A_j & B_j & C_j & & \\ & & & \ddots & \ddots & \ddots & \\ & & & & A_{J-1} & B_{J-1} & C_{J-1} \\ & & & & & A_J & B_J \end{bmatrix} \tag{88}$$

Each row of blocks corresponds to the set of governing equations at a point j. The block B_j contains the dependence of the equations on the state variables at the same grid point, and the A_j and C_j

blocks contain the dependence on the state variables at grid points $j-1$ and $j+1$ respectively. The formulas for each of these components are derived analytically from the governing equations, with the exception of the reaction rate terms, for which the derivatives are calculated numerically. While this is in principle a straightforward task, there are a number of subtleties that make actually calculating some of the terms a bit complex.

3.3.1 Numerically evaluated terms

The derivatives of the reaction rate terms are calculated using finite differences. In the energy equation, we require the derivatives of the production term $\dot{\omega}_k$ with respect to Y_i. We create a perturbed mass fraction vector $\mathbf{Y}'_i = [Y_0,, \ldots, Y_i + \epsilon, \ldots, Y_K]$

$$\frac{\partial \dot{\omega}_k}{\partial Y_i} = \frac{\dot{\omega}_k\left(\mathbf{Y}'_i, T\right) - \dot{\omega}_k\left(\mathbf{Y}, T\right)}{\epsilon} \tag{89}$$

and similarly

$$\frac{\partial \dot{\omega}_k}{\partial T} = \frac{\dot{\omega}_k\left(\mathbf{Y}, T + \epsilon\right) - \dot{\omega}_k\left(\mathbf{Y}, T\right)}{\epsilon} \tag{90}$$

In the energy equation, the derivatives with respect to species are computed in the same way, but the derivative with respect to temperature must be expanded since $\hat{h}_k$ also depends on T:

$$\frac{\partial}{\partial T}\left[\hat{h}_k \dot{\omega}_k\right] = \hat{h}_k \frac{\partial \dot{\omega}_k}{\partial T} + \hat{c}_{p,k} \dot{\omega}_k \tag{91}$$

The derivatives of the governing equations are taken term-by-term. A few terms that will be showing up repeatedly deserve special attention. As derived in Equation 74, the derivative of the density with respect to temperature is

$$\frac{\partial \rho_j}{\partial T_j} = -\frac{\rho_j}{T_j} \tag{92}$$

The derivative of the density with respect to mass fraction is a bit more complicated. We begin with the formula

$$\rho = \frac{P}{\bar{R}T_j}\left[\sum_i \frac{Y_i}{W_i}\right]^{-1} \tag{93}$$

Taking the derivative, this becomes

$$\frac{\partial \rho}{\partial Y_k} = -\frac{P}{\bar{R}T}\left[\sum_i \frac{Y_i}{W_i}\right]^{-2}\left(\frac{1}{W_k} + \sum_{i \neq k} \frac{1}{W_i}\frac{\partial Y_i}{\partial Y_k}\right) \tag{94}$$

$$\frac{\partial \rho}{\partial Y_k} = -\rho \bar{W}\left(\frac{1}{W_k} + \sum_{i \neq k} \frac{1}{W_i}\frac{\partial Y_i}{\partial Y_k}\right) \tag{95}$$

Assume that all of the Y_i (except for Y_k) vary proportionally, i.e.

$$\frac{1}{Y_i}\frac{\partial Y_i}{\partial Y_k} = \frac{1}{Y_j}\frac{\partial Y_j}{\partial Y_k} \tag{96}$$

and using the fact that $\sum Y_i = 1$, we find that

$$\frac{\partial Y_i}{\partial Y_k} = -\frac{Y_i}{1 - Y_k} \tag{97}$$

15

Substituting this into Equation 95, we find

$$\frac{\partial \rho}{\partial Y_k} = -\rho \bar{W} \left(\frac{1}{W_k} - \frac{1}{1-Y_k} \sum_{i \neq k} \frac{Y_i}{W_i} \right) \tag{98}$$

$$= -\rho \bar{W} \left(\frac{1}{W_k} - \frac{1}{1-Y_k} \sum_{i} \frac{Y_i}{W_i} + \frac{1}{W_k} \frac{Y_k}{1-Y_k} \right) \tag{99}$$

$$= -\rho \left(\frac{\bar{W}}{W_k} - \frac{1}{1-Y_k} + \frac{\bar{W}}{W_k} \frac{Y_k}{1-Y_k} \right) \tag{100}$$

$$\frac{\partial \rho}{\partial Y_k} = \frac{\rho \left(W_k - \bar{W} \right)}{W_k \left(1 - Y_k \right)} \tag{101}$$

All other quantities, such as transport coefficients and specific heats, are assumed to be constant for the purpose of evaluating the Jacobian, and the Soret mass flux is also ignored.

Sundials uses the Jacobian in the form

$$\mathbf{J} = \frac{\partial \mathbf{f}}{\partial \mathbf{y}} + \frac{1}{\tau} \frac{\partial \mathbf{f}}{\partial \mathbf{y}'} \tag{102}$$

where τ is the timestep. As an example, we give here the derivatives of the energy equation E_j, as all of the other equations are simpler.

$$E_j = \rho_j \frac{dT_j}{dt} + V_j \left(\mathbb{C}_j^- T_{,j-1} + \mathbb{C}_j T_{,j} + \mathbb{C}_j^+ T_{,j+1} \right) + \frac{1}{c_{p,j}} \sum h_{k,j} \dot{\omega}_{k,j}$$

$$+ \frac{1}{c_{p,j}} \frac{\mathcal{S}_j + \mathcal{S}_{j-1}}{2} \left(\mathbb{C}_j^- T_{,j-1} + \mathbb{C}_j T_{,j} + \mathbb{C}_j^+ T_{,j+1} \right) -$$

$$\frac{1}{r_j c_{p,j} \mathbb{D}_j} \left[r_{j+1/2} \left(\frac{\lambda_j + \lambda_{j+1}}{2} \frac{T_{j+1} - T_j}{h_j} \right) - r_{j-1/2} \left(\frac{\lambda_{j-1} + \lambda_j}{2} \frac{T_j - T_{j-1}}{h_{j-1}} \right) \right] \tag{103}$$

where

$$\mathcal{S}_j = - \sum_k \left(\frac{c_{p,k,j+1} + c_{p,k,j}}{2} \frac{\rho_j D_{km,j} + \rho_{j+1} D_{km,j+1}}{2} \frac{Y_{k,j+1} - Y_{k,j}}{h_j} \right) \tag{104}$$

In this equation, the Soret mass flux, the term containing the gradient in $\bar{W}$, and the correction mass flux j' have been neglected as their contributions are small. The blocks of the Jacobian are indicated as follows: The derivative of the kth equation with respect to the ith state variable at the jth grid point is written as $B_i^k(j)$, where we write U, T, and V as the subscripts and superscripts for those equations. The derivatives with respect to temperature are:

$$A_T^T(j) = V_j \mathbb{C}_j^- + \frac{\left(\mathcal{S}_j + \mathcal{S}_{j-1} \right) \mathbb{C}_j^-}{2c_{p,j}} - \frac{1}{r_j c_{p,j} \mathbb{D}_j} \left(\frac{r_{j-1/2}}{h_{j-1}} \frac{\lambda_{j-1} + \lambda_j}{2} \right) \tag{105}$$

$$B_T^T(j) = \frac{\rho_j}{\tau} - \frac{\rho_j}{T_j} \frac{dT_j}{dt} + V_j \mathbb{C}_j + \frac{1}{c_{p,j}} \sum_k \left(\hat{h}_{k,j} \frac{\partial \dot{\omega}_{k,j}}{\partial T} + \hat{c}_{p,k,j} \dot{\omega}_{k,j} \right) + \frac{\left(\mathcal{S}_j + \mathcal{S}_{j-1} \right) \mathbb{C}_j}{2c_{p,j}}$$

$$+ \frac{1}{r_j c_{p,j} \mathbb{D}_j} \left(\frac{r_{j+1/2}}{h_j} \frac{\lambda_j + \lambda_{j+1}}{2} + \frac{r_{j-1/2}}{h_{j-1}} \frac{\lambda_{j-1} + \lambda_j}{2} \right) \tag{106}$$

$$C_T^T(j) = V_j \mathbb{C}_j^+ + \frac{\left(\mathcal{S}_j + \mathcal{S}_{j-1} \right) \mathbb{C}_j^+}{2c_{p,j}} - \frac{1}{r_j c_{p,j} \mathbb{D}_j} \left(\frac{r_{j+1/2}}{h_j} \frac{\lambda_j + \lambda_{j+1}}{2} \right) \tag{107}$$

16

The derivatives with respect to species are:

$$A^T_{Y_k}(j) = \frac{1}{4c_{p,j}h_{j-1}} \left(c_{p,k,j} + c_{p,k,j-1}\right) \left(\rho_j D_{km,j} + \rho_{j-1} D_{km,j-1}\right) \left(\mathbb{C}^-_j T_{,j-1} + \mathbb{C}_j T_{,j} + \mathbb{C}^+_j T_{j+1}\right)$$

(108)

$$\begin{aligned} B^T_{Y_k}(j) = {}& \frac{\partial \rho_j}{\partial Y_k}\frac{dT_j}{dt} + \frac{1}{c_{p,j}}\sum_k \hat{h}_k \frac{\partial \dot{\omega}_{k,j}}{\partial Y_{k,j}} \\ & - \frac{1}{4c_{p,j}h_{j-1}} \left(c_{p,k,j} + c_{p,k,j-1}\right) \left(\rho_j D_{km,j} + \rho_{j-1} D_{km,j-1}\right) \left(\mathbb{C}^-_j T_{,j-1} + \mathbb{C}_j T_{,j} + \mathbb{C}^+_j T_{j+1}\right) \\ & - \frac{1}{4c_{p,j}h_j} \left(c_{p,k,j+1} + c_{p,k,j}\right) \left(\rho_{j+1} D_{km,j+1} + \rho_j D_{km,j}\right) \left(\mathbb{C}^-_j T_{,j-1} + \mathbb{C}_j T_{,j} + \mathbb{C}^+_j T_{j+1}\right) \end{aligned}$$

(109)

$$C^T_{Y_k}(j) = \frac{1}{4c_{p,j}h_j} \left(c_{p,k,j+1} + c_{p,k,j}\right) \left(\rho_{j+1} D_{km,j+1} + \rho_j D_{km,j}\right) \left(\mathbb{C}^-_j T_{,j-1} + \mathbb{C}_j T_{,j} + \mathbb{C}^+_j T_{j+1}\right)$$

(110)

The derivatives with respect to V are

$$B^T_V(j) = \mathbb{C}^-_j T_{,j-1} + \mathbb{C}_j T_{,j} + \mathbb{C}^+_j T_{j+1}$$

(111)

and all the derivatives with respect to U are zero.

3.4   Initial Condition

Integration of the system of equations requires a consistent set of initial conditions such that $\mathbf{f}\left(t_0, \mathbf{y}_0, \mathbf{y}'_0\right) = \mathbf{0}$. Physically, the initial condition is fully defined by the temperature, species mass fractions, and tangential velocity (U) profiles, along with the boundary value for the normal mass flux (V). From these, we must compute the time derivatives of T, Y_k, and U, as well as the value of V throughout the domain. These variables are all coupled in the governing equations, but since all of them appear linearly, their values may be found analytically. Start first by considering the continuity equation.

$$\frac{d\rho_j}{dt} + \frac{r^\alpha_j V_j - r^\alpha_{j-1} V_{j-1}}{r^\alpha_{j+1/2} h_{j-1}} + \rho_j U_j = 0$$

(112)

Now replace $d\rho/dt$ with equation 78 to obtain

$$-\frac{\rho_j}{T_j}\frac{dT_j}{dt} - \sum_k \frac{\rho_j \bar{W}_j}{W_k}\frac{dY_{k,j}}{dt} + \frac{r^\alpha_j V_j - r^\alpha_{j-1} V_{j-1}}{r^\alpha_{j+1/2} h_{j-1}} + \rho_j U_j = 0$$

(113)

Now, take the discretized energy and species equations, and write them as

$$\rho_j \frac{dT_j}{dt} = -V_j \frac{\partial T_j}{\partial r} - \mathbb{S}_{T,j}$$

(114)

$$\rho_j \frac{dY_{k,j}}{dt} = -V_j \frac{\partial Y_{k,j}}{\partial r} - \mathbb{S}_{k,j}$$

where $\mathbb{S}_{T,j}$ and $\mathbb{S}_{k,j}$ are the sums of the remaining terms in the respective equations. The continuity equation can then be rewritten as

$$\frac{1}{T_j}\left(V_j\frac{\partial T_j}{\partial r} + \mathbb{S}_{T,j}\right) + \sum_k \frac{\bar{W}_j}{W_k}\left(V_j\frac{\partial Y_{k,j}}{\partial r} + \mathbb{S}_{k,j}\right) + \frac{r^\alpha_j V_j - r^\alpha_{j-1} V_{j-1}}{r^\alpha_{j+1/2} h_{j-1}} + \rho_j U_j = 0$$

(115)

Solving for V_j gives

$$V_j = \frac{-\dfrac{\mathbb{S}_{T,j}}{T_j} - \displaystyle\sum_k \dfrac{\bar{W}_j}{W_k}\mathbb{S}_{k,j} - \rho_j U_j + \dfrac{r_{j-1}^\alpha V_{j-1}}{r_{j+1/2}^\alpha h_{j-1}}}{\dfrac{1}{T}\dfrac{\partial T_j}{\partial r} + \displaystyle\sum_k \dfrac{\bar{W}_j}{W_k}\dfrac{\partial Y_{k,j}}{\partial r} + \dfrac{r_j^\alpha}{h_{j-1}r_{j+1/2}^\alpha}} \tag{116}$$

This formula can be succesively applied to find V at each grid point from the boundary value at $j = 0$. Then, the time derivatives of the state variables are calculated from the governing equations:

$$\frac{dT_j}{dt} = -\frac{1}{\rho_j}\left(V_j\frac{\partial T_j}{\partial r} + \mathbb{S}_{T,j}\right) \tag{117}$$

$$\frac{dY_{k,j}}{dt} = -\frac{1}{\rho_j}\left(V_j\frac{\partial Y_{k,j}}{\partial r} + \mathbb{S}_{k,j}\right) \tag{118}$$

3.5 Flame Radius Control

To simulate flames at a specific radius of curvature, a mechanism must be implemented to provide control over the flame location. In the elemental flame formulation, the flame radius is controlled by manipulating the mass flux per radian $(rV)_0$ at the $r = 0$ boundary. This is expressed in terms of a fictitious non-reacting stagnation point radius R.

$$(rV)_0 = \frac{a}{2}\rho_0\,|R|\,R \tag{119}$$

The current flame radius is defined as

$$R_f \equiv \frac{\int_0^\infty q'''r\,dr}{\int_0^\infty q'''\,dr} \tag{120}$$

THIS IS NO LONGER CORRECT Given a target flame radius R_f^*, a PI (proportional–integral) control algorithm is applied to the stagnation point radius to determine the value of the centerline mass flux.

$$R = K_1\left[\left(R_f^* - R_f\right) + K_2\int\left(R_f^* - R_f\right)dt\right] \tag{121}$$

Appropriate values of the controller gains K_1 and K_2 depend on the characteristics of the flame being simulated. For the flames presented here, acceptable values of the gains are $K_1 = 10$ and $K_2 = 800\,\mathrm{s}^{-1}$.

3.6 Adaptation and Regridding

A number of grid adaptation criteria are applied to ensure accurate solution of the discretized problem with a minimum number of grid points. The following criteria must be met between each pair of grid points. If any of these criteria are not met, a new grid point is introduced midway between the two existing points.

First, the grid must accurately resolve variations in the scalar quantities relative to their respective ranges.

$$|F_{j+1} - F_j| < \varphi_1\left(\max_j F - \min_j F\right) \tag{122}$$

18

where F includes each of the dependent variables T, Y_k, U, V as well as the chemical source term $\sum h_k \dot{\omega}_k W_k$, and φ_1 is a tolerance parameter on the order of 0.1. Gradients of the scalar quantities are subject to an similar criterion

$$\left| \left(\frac{\partial F}{\partial r} \right)_{j+1} - \left(\frac{\partial F}{\partial r} \right)_j \right| < \varphi_2 \left(\max_j \frac{\partial F}{\partial r} - \min_j \frac{\partial F}{\partial r} \right) \tag{123}$$

where the tolerance parameter φ_2 has a typical value of 0.3.

THIS PART IS NO LONGER CORRECT The next criterion ensures that numerical diffusion and dispersion introduced by the discretization of the convection terms in the conservation equations is small compared to the physical diffusion terms

$$x_{j+1} - x_j < \varphi_3 |d_j| \tag{124}$$

where the damping ratio d_j is $\rho D_{km}/V$ for the species equation, $\lambda/c_p V$ for the energy equation and μ/V for the momentum equation. The tolerance parameter φ_3 has a typical value of 1.0. The final grid adaptation criterion forces the grid to be relatively uniform.

$$\varphi_4 < \frac{x_{j+1} - x_j}{x_j - x_{j-1}} < \frac{1}{\varphi_4} \tag{125}$$

φ_4 has a value of around 2.5. If all of these criteria are met to better than their required tolerance without a particular grid point, then that grid point may be safely removed.

The location of the boundary grid points is also modified dynamically. For the sake of computational efficiency, the computational domain should be truncated as close to the flame as possible while still resolving the complete flame structure. That is, we expect that $\partial F/\partial x \to 0$ as $r \to \pm\infty$ even when using fixed-value boundary conditions. This condition may be written at the right $(j = J)$ boundary for a scalar F as

$$|F_J - F_{J-2}| < \varphi_5 \left(\max_j F - \min_j F \right) \tag{126}$$

where the tolerance parameter φ_5 is typically chosen on the order of 10^{-4}. Note that the boundary value must be compared with the value two grid points away since the flatness criterion between J and $J-1$ is sometimes satisfied exactly by an imposed zero-gradient boundary condition.

4 Code Description

(work in progress)

This section is the link between the equations described above and the actual C++ implementation of the 1D flame code. It should include tables that pair up the variable names in code with the variables used in the above. This section should also contain a description of the input file format, and compilation instructions on supported platforms.

Name in code	Name here	Description	Units	Eq.
j	j	grid point index	-	
jj	J	index of the rightmost grid point	-	
k	k	species index	-	
nSpec	K	number of species	-	
T[j]	T_j	temperature	K	
U[j]	U_j	normalized tangential velocity	s^{-1}	
V[j]	V_j	normal mass flux	$\mathrm{kg/m}^2 \cdot \mathrm{s}$	
Y(k,j)	$Y_{k,j}$	species mass fractions	-	
rho[j]	ρ_j	density	$\mathrm{kg/m}^3$	
W[k]	W_k	molecular weight of species k	kg/kmol	
Wmx[j]	$\bar{W}_j$	mixture molecular weight	kg/kmol	
sumcpj[j]	$\mathcal{S}_j$	enthalpy flux	$\mathrm{W/m}^2 \cdot \mathrm{K}$	64, 104
mu[j]	μ_j	dynamic viscosity	$\mathrm{Pa} \cdot \mathrm{s}$	
lambda[j]	λ_j	thermal conductivity	$\mathrm{W/m} \cdot \mathrm{K}$	
cp[j]	$c_{p,j}$	mixture specific heat	$\mathrm{J/kg} \cdot \mathrm{K}$	
cpSpec(k,j)	$\hat{c}_{p,k,j}$	species molar specific heat	$\mathrm{J/kmol} \cdot \mathrm{K}$	
qFourier[j]	q_j	heat flux	$\mathrm{W/m}^2$	62
rhoD(k,j)	$\rho_j D_{km,j}$	density-weighted diffusion coefficient	$\mathrm{kg/m} \cdot \mathrm{s}$	
Dkt(k,j)	$D^T_{k,j}$	thermal diffusion coefficient	m^2/s	
jCorr[j]	j'_j	correction to diffusion mass flux	$\mathrm{kg/m}^2 \cdot \mathrm{s}$	

References

R. J. Kee, M. E. Coltrin, and P. Glarborg. *Chemically Reacting Flow: Theory and Practice*. Wiley, New York, 2003.

Y. M. Marzouk. The effect of flow and mixture inhomogeneity on the dynamics of strained flames. Master's thesis, Massachusetts Institute of Technology, August 1999.

Y. M. Marzouk, A. F. Ghoniem, and H. N. Najm. Toward a flame embedding model for turbulent combustion simulation. *AIAA Journal*, 41(4):641–652, 2003.